

Reaction between Gas-phase Hydrogen Atom and Chemisorbed Bromine Atoms on a Silicon(001)-(2×1) Surface

Jongkeun Park, Jongbaik Ree,* Sang Kwon Lee, and Yoo Hang Kim†

Department of Chemistry Education, Chonnam National University, Gwangju 500-757, Korea. *E-mail: jbre@chonnam.ac.kr

†Department of Chemistry and Center for Chemical Dynamics, Inha University, Incheon 402-751, Korea

Received July 12, 2007

The reaction between gas-phase atomic hydrogen and highly covered chemisorbed bromine atoms on a silicon(001)-(2×1) surface is studied by use of the classical trajectory approach. The model is based on reaction zone consisting of H, Br and Si atom interacting with a finite number of primary system silicon atoms, which are coupled to the heat bath. The calculations were carried out in the temperature range 300-2500 K for the gaseous H atom and 0-700 K for the surface, respectively. All reactive events occur in a single impact collision on a subpicosecond scale, following the Eley-Rideal mechanism. The reaction probability is dependent upon the gas temperature and the largest near 800 K, but it is essentially independent of the surface temperature. The reaction energy available for the product state is small, and most of the reaction exothermicity deposits in vibration and translation of the product, HBr molecule.

Key Words : Collision-induced, Hydrogen, Chemisorbed bromine, Silicon

Introduction

In the past four decades, researchers have shown that it is possible to direct gas-phase reactants toward adsorbed species on well characterized surfaces and to determine the outcome of interaction events by use of spectroscopic techniques.¹⁻³ Such studies have given valuable insight into the chemical and physical properties of adsorbed layers, and are essential for the development of fundamental concepts on gas-surface reactions. In gas-atom interaction taking place on a solid surface, important reactive events involve the dissociation of the adatom-surface bond and association of the gas atom with the desorbing adatom. Such interactions are often highly exothermic, so there is a large amount of energy to be deposited in the various motions of the product. For example, chemisorption energies of atoms such as hydrogen and chlorine on a close-packed metal surface lie in the range of 2-3 eV,^{4,5} whereas the energy of the bond formed between such atoms is 4-5 eV.⁶ Thus, the reaction exothermicity is about 2 eV, which is to be distributed among various motions of the product and the solid phase. So far, most studies have been performed on these types of reaction, that is, the highly exothermic reactions. The exothermicity is still very significant in the reactions involving a nonmetallic surface such as graphite and silicon as well.⁷⁻¹³ We have studied the reaction of gas-phase chlorine or hydrogen atom with highly covered chemisorbed hydrogen atoms on a silicon surface, and reported that the mechanism of the reactions is the Eley-Rideal type.^{12,13} We also have studied the reaction of gas-phase bromine atom with highly covered chemisorbed hydrogen atoms on a silicon surface, in which the reaction is slightly endothermic, and reported that the mechanism of the reactions is also the Eley-Rideal type.^{14,15}

In the present paper, we have studied the reaction of gas-phase hydrogen atom with a Br-saturated silicon surface.

Especially, we have addressed what the reaction mechanism of gas-phase atomic hydrogen with chemisorbed bromine atoms on silicon(001)-(2×1) surface is in the case of high surface coverage. In this model, one bromine atom is adsorbed on each silicon atom on the surface. To study the reaction, we have followed the time evolution of the pertinent coordinates and conjugate momenta of each reactive trajectory on a London-Eyring-Polanyi-Sato (LEPS) potential energy surface, which is constructed with many-body interactions operating between all atoms of the reaction system. The time evolution of the trajectories was determined by solving the equations of motion formulated by uniting gas-surface procedure and generalized Langevin theory for the solid phase.^{16,17}

Interaction Model

The interaction model and the numerical procedures have already been reported in detail in Ref. 12. The interaction model is the same as the one in Ref. 12 except that the chlorine atom is now replaced by the bromine atom. We summarize the essential aspects of the interaction and the numerical procedures on the silicon (001)-(2×1) surface reconstructed by forming dimers along the [110] direction [Figure 1(a)]. For easy reference we have displayed the collision model in Figure 1(b). The Br atom is chemisorbed on the Si atom of the symmetric dimer structure. This Si atom is the zeroth member of the (N+1)-atom chain which links the reaction zone to the heat bath. Furthermore, the zeroth Si atom is surrounded by eight nearby Si atoms identified by numbers 1, 2, ..., 8 in Figure 1(b). The reaction zone atoms are the zeroth Si atom, the adatom, Br, and the incident H atom. We consider that these reaction zone atoms, eight surrounding Si atoms, and the N-chain atoms constitute the primary system. We then designate the remaining infinite

1.6 ± 0.2 kcal/mole.^{23,24} After systematically varying the values of the Sato parameter Δ 's, we find that the set $\Delta_{\text{HBr}} = 0.10$, $\Delta_{\text{BrSi}} = 0.08$ and $\Delta_{\text{HS}} = 0.37$ for the H to the surface Si atoms, describe best the desired features, minimizing the barrier height and the attractive well in the product channel.

Once the potential energy surface (PES) is determined, we can follow the time evolution of the primary system by integrating the equations of motion, which describe the motions of the reaction zone atoms and N -chain atoms. We expect that this PES will enable us to understand how gas atom and adsorbate atom react with each other and then depart from the surface. An intuitive way to treat the dynamics of the reaction involving many surface atoms is to solve a united set of equations of motion for the reaction zone atoms and the Langevin equations for N -chain atoms, which couple the reaction zone to the heat bath. The gas-atom part of the resulting equations are $m_i \ddot{Y}_i(t) = -U/\partial Y_i$, where $Y_1 = z$, $Y_2 = \rho$, $Y_3 = \Phi$, $Y_4 = r_{\text{BrSi}}$, $Y_5 = \theta$, $Y_6 = \phi$, with $m_1 = m_{\text{H}}$, $m_2 = \mu_{\text{HBr}}$, $m_3 = I_{\text{HBr}}$, $m_4 = \mu_{\text{BrSi}}$, $m_5 = m_6 = I_{\text{BrSi}}$. Here μ_i and I_i are the reduced mass and the moment of inertia of the interaction system indicated. For the $(N+1)$ -atom chain, which includes the zeroth Si atom, the equations are

$$M_s \ddot{\xi}_0(t) = -M_s \omega_{e0}^2 \xi_0(t) + M_s \omega_{c1}^2 \xi_1(t) - \partial U(z_{\text{BrSi}}, \theta, \phi, \rho, Z, \Phi, \{\xi\}) / \partial \xi_0 \quad (2a)$$

$$M_s \ddot{\xi}_j(t) = -M_s \omega_{ej}^2 \xi_j(t) + M_s \omega_{cj}^2 \xi_{j-1}(t) + M_s \omega_{e,j+1}^2 \xi_{j+1}(t), j = 1, 2, \dots, N-1 \quad (2b)$$

$$M_s \ddot{\xi}_N(t) = -M_s \Omega_N^2 \xi_N(t) + M_s \omega_{c,N}^2 \xi_{N-1}(t) - M_s \beta_{N+1} \dot{\xi}_N(t) + M_s f_{N+1}(t) \quad (2c)$$

Equation (2a) is for the vibration of the zeroth chain atom on which the Br atom is chemisorbed. Equation (2c) is for the vibration of the N th atom which is bound to the bulk phase. The N th Si is directly linked to the heat bath, and through this coupling the heat bath exerts systematic dissipative and random (or stochastic) forces on the primary system composed of the reaction zone atoms and the N -chain atoms. Ω_N is the adiabatic frequency. The friction coefficient β_{N+1} is very close to $\pi\omega_D/6$, where ω_D is the Debye frequency, and governs the dissipation of energy from the primary zone to the heat bath. The Debye temperature is 640 K.²⁵ All values of β , ω_e , ω_c , and Ω are presented elsewhere.²⁶ The quantity $M_s f_{N+1}(t)$ is the random force on the primary system arising from thermal fluctuation in the heat bath. This force balances, on average, the dissipative force, $M_s \beta_{N+1} \dot{\xi}_N(t)$, which removes energy from the $(N+1)$ atom chain system in order that the equilibrium distribution of energies in the chain can be restored after collision.

The computational procedures make use of Monte Carlo routines to generate random numbers for the initial conditions. The first of them is the collision energies E sampled from a Maxwell distribution at the gas temperature T_g . In sampling impact parameters b , we note that the distance between the bromine atoms adsorbed on the nearest Si sites

is 3.79 Å. Thus, we take the half-way distance so that the flat sampling range is $0 \leq b \leq 1.90$ (i.e., $b_{\text{max}} = 1.90$ Å). In the collision with $b > 1.90$ Å, the gas atom is now in the interaction range of the bromine atom adsorbed on the adjacent surface site. The initial conditions and numerical techniques needed in solving the equations of motions are given in detail elsewhere.^{12,13} To ascertain what really happens during the reaction, we followed each trajectory for sufficiently long time, 50ps.

Results and Discussion

Reaction probabilities. Since the typical experimental condition for producing hydrogen atoms is 1800 K,²⁷ we considered the reaction occurring at the gas temperature of 1800 K. At the thermal conditions of $(T_g, T_s) = (1800, 300$ K), for the total number of 40000 trajectories sampled, the reaction probability for the primary reaction pathway, HBr formation, is found to be 0.0516. The reaction probability at the chosen gas and surface temperature (T_g, T_s) is defined as the ratio of the number of reactive trajectories N_R to the total number of trajectories $N_T (= 40,000)$ sampled over the entire range of impact parameters. This result is similar to that for H(g) interacting with Cl(ad)/Si¹² or H(D)(g) interacting with D(H)/Si,^{7,28,29} in that the primary reaction pathway is the gas phase molecule, i.e., HCl(g) or HD(g), formation. Especially, HBr formation probability is close to the HCl formation probability ($P = 0.088$).¹²

We first consider the distribution of reaction times t_R at the thermal conditions of $(T_g, T_s) = (1800, 300$ K). Out of $N_T = 40000$ trajectories sampled at this thermal condition, $N_R = 2064$ are reactive. All these reactive events are found to occur on a sub-picosecond time scale through a single gas-surface collision. The ensemble average of reaction times is 0.46 ps. Thus these results clearly suggest the ER mechanism, in which the incident atom cannot accommodate to the surface temperature since it is not trapped. The probability $P(T_g, T_s)$ defined above is a total probability at the thermal conditions of T_g and T_s . However, it is instructive to analyze the dependence of the extent of reaction on the impact parameter. To determine the probability of reaction as a function of the impact parameter, $P(T_g, T_s; b)$, we count reactive trajectories in intervals of $b = 0.050$ Å and divide that number $N_R(b)$ by the number of collisions taking place in the interval, $N(b)$. For example, the number of trajectories sampled between $b = 0$ and 0.050 Å is $N(b) = 1005$, of which $N_R(b) = 424$ are reactive. The probability $P(T_g, T_s; b)$ is then the ratio $N_R(b)/N(b) = 0.422$ and this value is plotted at the midpoint 0.025 Å in Figure 2(b). As shown in Figure 2(b), the probability $P(T_g, T_s; b)$ takes its maximum value at $b \approx 0$ and then decreases as b increases. At $b = 0.275$ Å, it is about 0.17 and the reaction ceases near $b = 0.5$ Å. The same general trend was found in H+Cl/Si system too. If the adjacent surface sites are also occupied by Br atoms, the nearest Br-to-Br distance is $d_{\text{BrBr}} = 3.79$ Å so the half-way distance $1/2 d_{\text{BrBr}}$ is much greater than the impact parameter 0.5 Å for the reaction range. Therefore, the reaction occurs

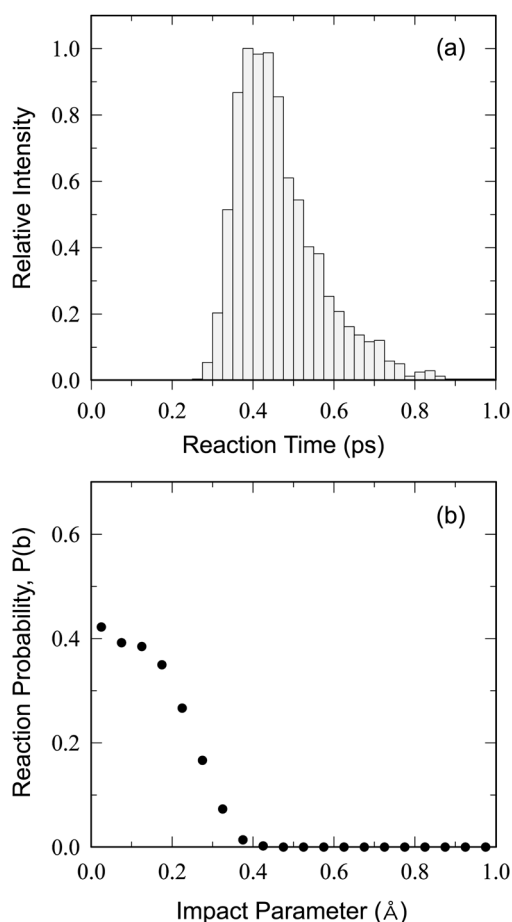


Figure 2. (a) Reaction time distribution. (b) Dependence of the reaction probability $P(b)$ on the impact parameter. Both figures are for the thermal condition ($T_g = 1800$, $T_s = 300$ K).

in a localized region around the adatom site on the surface. Such localized reactivity has been observed in the hydrogen abstraction reaction on silicon by gas-phase atomic hydrogen (H or D).²⁷ Thus even if the surface coverage is high, the formation of HBr is not expected to be much influenced by nearby bromine atoms. In such a case, those gas atoms approaching the target Br atom in Figure 1(b) with $b \geq \frac{1}{2}d_{\text{BrBr}}$ are now in the interaction range of Br adsorbed on the adjacent surface site. From the b -dependent reaction probability we obtain the total reaction cross section of 0.0897 \AA^2 using the expression defined as $\sigma = 2\pi \int_0^{b_{\text{max}}} P(T_g, T_s; b) b db$, where b_{max} is 1.90 \AA . The total cross section is small, in part reflecting the occurrence of reactive events only in the immediate neighborhood of the adatom and the small value of the reaction probability itself. This reaction cross section is smaller than that of the related system $\text{H(g)} + \text{Cl(ad)/Si}$ (*i.e.*, 0.165 \AA^2).¹² The reason why the reaction cross section for $\text{H} + \text{Br/Si}$ system is smaller than that for $\text{H} + \text{Cl/Si}$ is that $P(b)$ values for the former are generally lower than those for the latter.

Temperature dependence of reaction probabilities. Plotted in Figure 3(a) is the reaction probability $P(T_g, T_s)$ as a function of the surface temperature from 0 to 700 K at $T_g = 1800$ K. Over the whole surface temperature range con-

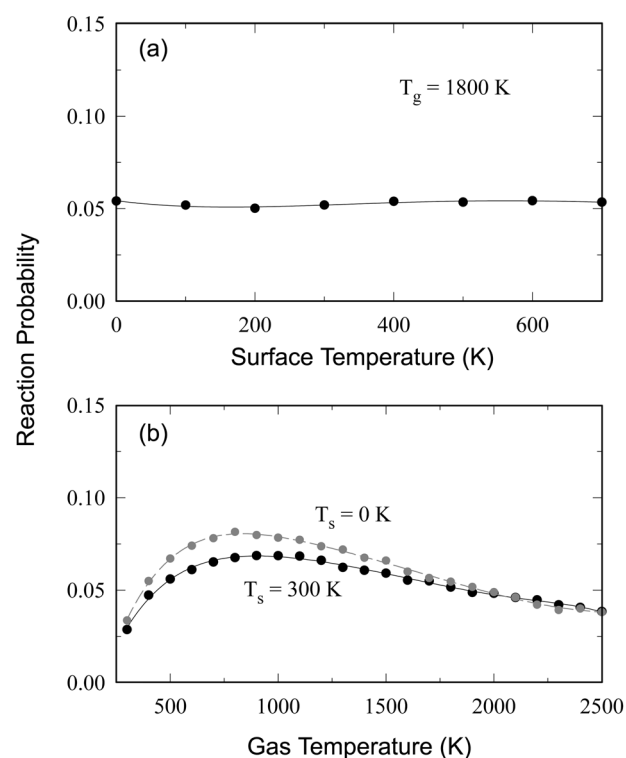


Figure 3. Dependence of the reaction probability $P(T_g, T_s)$ on the gas and surface temperatures. (a) Dependence on the surface temperature when the gas temperature is fixed at 1800 K. (b) Dependence on the gas temperature when the surface temperature is fixed at 0 K (open circles) and 300 K (filled circles).

sidered in the study, calculated reaction probabilities remain close to 0.05. Such a significant value of the reaction probability at the low end of the T_s range implies that the reaction proceeds over a small activation energy barrier, an important feature for an ER reaction. The magnitude of the reaction probability, as well as its temperature dependence, is comparable to those of the atomic H abstraction reaction in $\text{H(g)} + \text{H(ad)/Si}$.⁷ It is interesting to note that although the mass distributions are different, the basic energetics of these two reactions are very similar. As noted above, $D_{0, \text{HBr}}^0 = 3.76 \text{ eV}$, which is close to $D_{0, \text{H}_2}^0 = 4.48 \text{ eV}$. For the adatom-surface interactions Br(ad)/Si and H(ad)/Si , the dissociation energies are $D_{0, \text{BrSi}}^0 = 3.59 \text{ eV}$ and $D_{0, \text{HSi}}^0 = 3.36 \text{ eV}$, which are also very close to each other. Figure 3(a) shows that the effect of surface temperature on the reaction is negligible, which is a typical result for an ER process. Such a negligible effect of the silicon surface temperature on the extent of halogen extraction processes has already been noted in ref. 12. The weak temperature dependence shown in Figure 3(a) also suggests that the driving force for the Br extraction reaction resides in the high potential energy of atomic hydrogen.

The dependence of the reaction probability on the gas temperature is much stronger than the T_s dependence shown in Figure 3(a). The results presented in Figure 3(b) for a fixed surface temperature of 0 and 300 K show that the reaction probability rises rapidly with the gas temperature in

the range of $T_g = 300$ to 800 K, beyond which it decreases slowly with increasing temperature. The variation of reaction probability at lower temperatures follows the “normal” thermal effect that the extent of a chemical reaction increases with increasing temperature. At higher temperatures, where high energy collisions dominate, however, the fast moving gas atom does not stay on the surface long enough to cause reaction. Thus a larger fraction of trajectories leave the surface without reaction, so the reaction probability decreases at high temperatures, exhibiting an “inverse” temperature dependence.

We note here the effects of initial vibrational states of the Br(ad)-Si bonds. In all calculations, we have sampled the initial energy of the Br-Si vibration, $E_{v_{BrSi}}^0$, corresponding to quantum numbers $v_{BrSi} = 0, 1, 2, \dots$, weighted by a Boltzmann distribution at the surface temperature. The contribution coming from higher vibrational states ($v_{BrSi} > 0$) is only important at higher surface temperatures (>300 K). At $(1800, 300$ K), the values for $P_{v_{BrSi}}(T_g, T_s)$ for $v_{BrSi} = 0, 1, 2$, and 3 are $0.0512, 0.0524, 0.0535$, and 0.0543 , respectively, showing a very weak dependence on the initial excitation of the adatom-surface vibration. This very weak dependence is mainly due to small vibrational spacing. The Br-Si stretching of the inclined bond is only 500 cm^{-1} or 62 meV .²¹ The initial vibrational energies corresponding to $v_{BrSi} = 0, 1, 2$, and 3 are $0.031, 0.093, 0.155$, and 0.217 eV , respectively. When the Boltzmann population of initial vibrational states is used, the contribution coming from the excited Br-Si vibrational states is not important in the present system, since essentially all of the Br-Si vibrations are in the ground state. For example, at $T_s = 300$ K, the fractions of the Br-Si vibration in $v_{BrSi} = 0, 1$, and 2 are $0.909, 0.083$, and 0.0075 , respectively. Therefore, the difference between the reaction probability calculated with the Boltzmann distribution of the Br-Si vibration and that with $v_{BrSi} = 0$ is negligible. In fact, for these two cases of the Br-Si vibrational state, the reaction probabilities at $T_g = 1800$ K and $T_s = 300$ K are 0.0516 and 0.0512 , respectively.

The dependence of the reaction probability on the initial excitation of the Br-Si vibration is very different from the $\text{H(g)} + \text{H(ad)/Si}$ system, where increasing the initial vibrational state of the adsorbate from $v = 0$ to $v = 1$ nearly doubles the reaction probability.⁷ This difference is due to the different mass distribution. The latter reaction involves the light-light-heavy (**L+LH**) mass distribution, whose kinematics is very different from the present (**L+HH**) distribution despite the similar energetics as noted above.¹²

Energy partitioning. The exothermicity of the gas-phase $\text{H+Br} \rightarrow \text{HBr}$ is $D_0^0 = 3.76\text{ eV}$ (or 363 kJ/mol), whereas D_0^0 for the Br-Si surface is 3.59 eV . In the ER reaction, the reactant state is H(g)+Br(ad) , which is thus about 0.17 eV above the HBr(g) state, *i.e.*, the reaction to form HBr(g) is exothermic by this amount. Other energies available for the product state are the collision energy of the incident gas atom E , the initial energy of the Br-Si vibration and the initial energy of the solid. For example, when $T_s = 0$ K, the exothermic reaction energy available for the product state

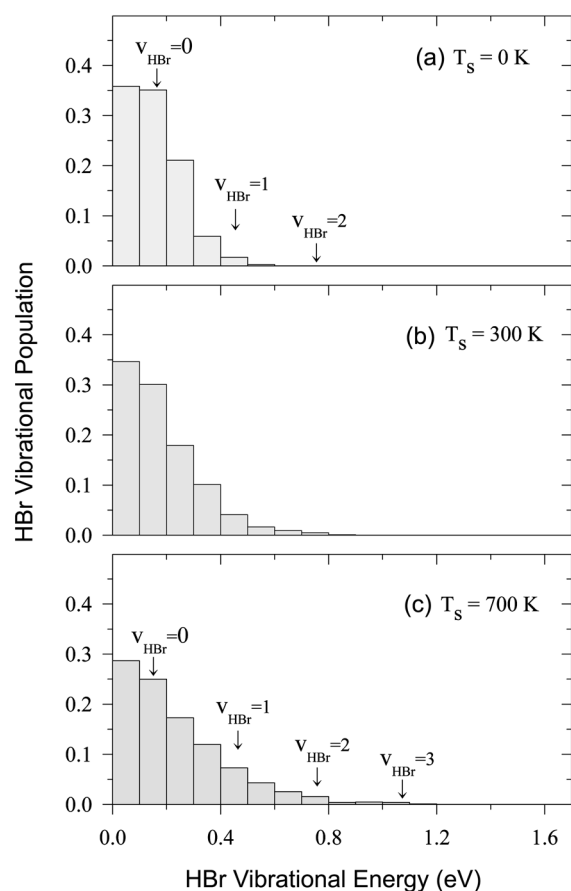


Figure 4. Relative distribution of HBr vibrational states at the surface temperature (a) 0 K, (b) 300 K, and (c) 700 K. The gas temperature is fixed at 1800 K. The vibrational energies corresponding to $v_{HBr} = 0, 1, 2$, and 3 are indicated.

after breaking the Br-Si bond is only $(0.17+E)\text{ eV}$, so vibrational excitation of HBr is not expected to be high in this reaction, except for the collisions which occur in the high velocity tail section of the Maxwell distribution of collision energies. This situation is very different from $\text{H(g)} + \text{H(ad)/W}$ or O(g)+H(ad)/W , where the available energy is in excess of 2 eV .^{30,31} In O(g)+CO(ad)/Pt , the available energy is as large as 4 eV .²⁶ In these heavy atom surface systems, almost all of the excess energy could end up in the gas-phase molecular product.

The relative distributions of vibrational population for HBr at $T_s = 0, 300$, and 700 K are shown in Figure 4. Here, the gas temperature is maintained at 1800 K. The figures show bar graphs for the ratio of the number of reactive trajectories in intervals of 0.10 eV to the total number of reactive trajectories N_R as a function of the vibrational energy of the product molecule HBr. The plot indicates that the vibrational population distribution in the present reaction is statistical, especially on the cold surface. This variation is similar to that of the ER component of gas-phase atomic hydrogen reacting with chemisorbed chlorine atoms on the gold³² and silicon¹² surface. The variation, however, is radically different from the result of atomic oxygen reacting with chemisorbed hydrogen atoms on a tungsten surface,

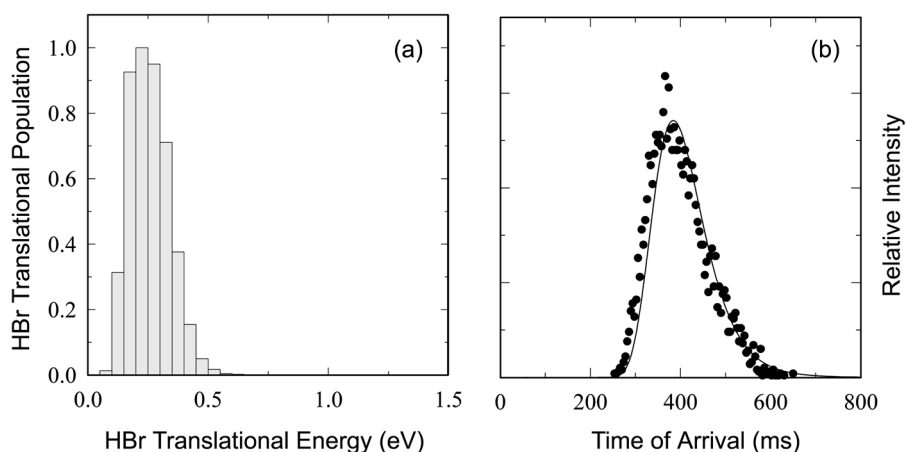


Figure 5. (a) Translational population distribution of HBr. (b) Time-of-flight distribution for HBr from the surface. Both figures are for the thermal condition (1800, 300 K).

where product OH can be in a highly excited state with a vibrational population inversion.³¹ In the latter reaction, the exothermicity is much larger than the present reaction (*i.e.*, $D_{\text{OH}} = 4.624$ eV but D_{HW} is only 2.30 eV). From the eigenvalue expression $E_{\text{vib}}(v_{\text{HBr}}) = hc\omega_e(v_{\text{HBr}} + 1/2) - hc\omega_e x_e(v_{\text{HBr}} + 1/2)^2$ with $\omega_e = 2649$ cm^{-1} and $\omega_e x_e = 45.22$ cm^{-1} ,¹⁹ we find the vibrational energies 0.163, 0.489, 0.786, and 1.081 eV for $v_{\text{HBr}} = 0, 1, 2,$ and $3,$ respectively. The comparison of these energies with the energy scale used in Figure 4 indicates that the majority of product molecules have their vibrational energies roughly corresponding to $v_{\text{HBr}} = 0$. However, the production of HBr with the vibrational energy corresponding to $v_{\text{HBr}} = 1$ increases significantly as the surface temperature increases, even though the reaction probability itself remains essentially unchanged [see Figure 2(a)]. When $T_s = 700$ K, a small fraction of molecules with a vibrational energy near 1.0 eV, which is close to the $v_{\text{HBr}} = 3$ level, are produced from the reactive events involving the Br-Si vibration in an excited state. At this surface temperature, the fractions of the Br-Si vibration in $v_{\text{BrSi}} = 0, 1, 2,$ and 3 are 0.653, 0.234, 0.084, and 0.030, respectively.

The amount of energy deposited in the translational motion of HBr at (1800, 300 K) is somewhat larger than the vibrational energy [compare Figures 4(b) and 5(a)]. The ensemble-averaged translational energy is 0.258 eV, whereas the ensemble average of the vibrational energy displayed in Figure 4(b) is 0.178 eV. This figure shows the diminished number of reactive events with translational energy less than about 0.2 eV. In this case, more energy is deposited in the vibrational motion. Thus, such vibrationally excited molecules leave the surface more slowly. Figure 5(b) shows a time-of-flight distribution of product molecules along with the fitted curve. The points are obtained by collecting molecules reaching the “reaction chamber-to-detector” distance of 30 cm. A smooth distribution of product velocities indicates the occurrence of a single type of reactive collision, namely, the direct-mode collision. The distribution fits well with a velocity function of the form³³ $f(v) = A v^3 e^{-(v-v_0)^2/\alpha^2}$ with $A = 3.94 \times 10^{-8}$, $v_0 = 1457$ m/s and $\alpha = 330$ m/s, where

A is the normalization constant. The velocity distribution takes the maximum value at $v_{\text{max}} = 1/2[v_0 + (v_0^2 + 6\alpha^2)^{1/2}] = 1561$ m/s, which gives $1/2 m_{\text{HBr}} v_{\text{max}}^2 = 0.890$ eV. This energy is very large compared to $3/2kT_g = 0.233$ eV, indicating that the velocity distribution is highly non-Boltzmann.

It is interesting to compare the energy distribution in the present reaction H(g)+Br(ad)/Si with that of the related reaction Br(g)+H(ad)/Si.¹⁴ Even though two reactions have very different mass distributions, the vibrational energy distribution of the product HBr is very similar, *i.e.*, statistical for both systems. This is because the reaction exothermicities are similar, nearly zero or even slightly negative. Both reactions are driven by the reaction exothermicities of similar small magnitude. Therefore, vibrational excitation is very limited and vibrational distribution is statistical for both systems.

The amount of energy taken up by the rotational motion of HBr molecule is very small, in contrast to the translational and vibrational motions. Here, the rotational energy is calculated as $E_{\text{HBr,rot}} = L^2/(2\mu_{\text{HBr}}r_{\text{HBr}}^2)$, where the angular momentum $L = \mu_{\text{HBr}}(z\dot{\rho} - \rho\dot{z})$ with the corresponding quantum number $J = L/\hbar$. As in the above-discussed vibrational quantum number, the rotational quantum number J_{HBr} corresponding to the rotational energy E_{rot} can be calculated through the relation $J_{\text{HBr}} = \text{int}[E_{\text{rot}}/E_{\text{rot}}(J_{\text{HBr}})]$, where $E_{\text{rot}}(J_{\text{HBr}}) = J_{\text{HBr}}(J_{\text{HBr}}+1)\hbar^2/2I_{\text{HBr}}$. The maximum occurs at $J_{\text{max}} = 0$ [see Figure 6(a)]. If we take the gas temperature of 1800 K, the rotational maximum obtained from the Boltzmann expression $J_{\text{max}} = 1/2[(2kT/\bar{B})^{1/2} - 1]$ with $\bar{B} = 8.46$ cm^{-1} is 8. On the other hand, for the surface temperature of 300 K, the Boltzmann intensity peaks at $J_{\text{max}} = 3$. The shape and intensity distribution of the present calculation show that the rotational states of product HBr are shifted to much lower J side compared to the Boltzmann distribution even at $T_g = 300$ K. In addition to this rotational population distribution, it is interesting to know how the desorbing HBr molecules are rotationally aligned at the instant of desorption. To examine this aspect, we have calculated the angle between the axis of rotation of HBr and the surface normal when the

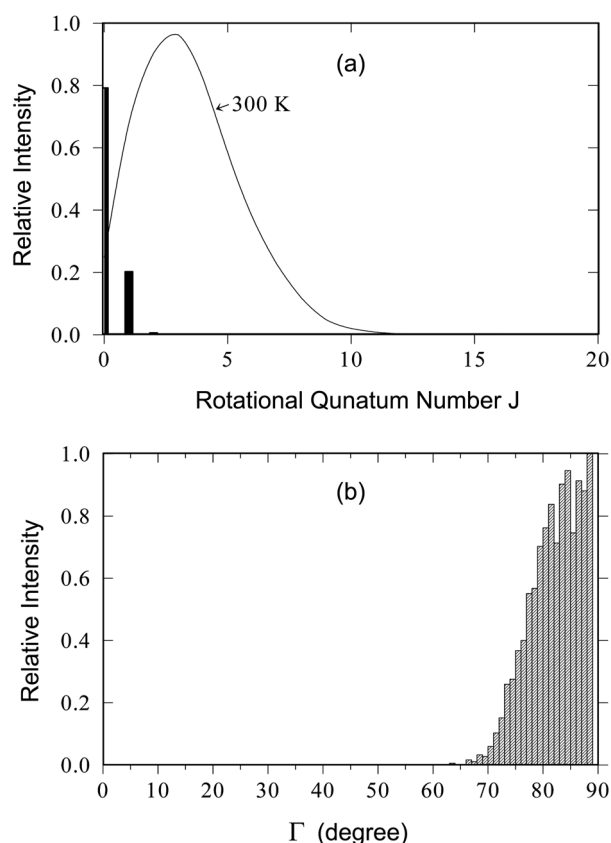


Figure 6. (a) Relative intensity of the rotational population distribution of HBr. The solid curve is the Boltzmann distribution at 300 K. (b) Distribution of the angle between the axis of HBr rotation and the surface normal, Γ .

H atom turns the corner after the final impact and begins the journey outward with Br. The angular distribution is found to be sharply peaked near 90° , indicating that the rotational axis is closely parallel to the surface [see Figure 6(b)]. That is, the product molecules leave the surface in a cartwheel-like rotation.

The ensemble-averaged energy transfer to the silicon surface $\langle E_s \rangle$ at (1800, 300 K) is 0.168 eV, which means that the solid surface gains energy after collision. In other systems such as H+H/Si and Cl+H/Si, the $\langle E_s \rangle$ values are approximately 0.1 eV,^{13,34} which is similar to the present system. In Br+H/Si system, however, the reaction is slightly endothermic and $\langle E_s \rangle$ is negative reflecting the fact that the system must gain energy from the surface for the endothermic reaction to occur.¹⁴

Representative trajectory. In Figure 7(a), we plot the time evolution of H-surface, H-Br, and Br-Si distances for a representative case at (1800, 300 K). The oscillatory behavior of the H-surface distance after the first minimum is the imprint of the H-Br vibration. The latter situation can be readily noticed by comparing its oscillatory period with the vibrational period of the HBr distance. The first minimum of the H-surface represents the impact of the H atom with the surface in this single turning point collision. From $t = -\infty$ to the turning point which occurs near $t = 0$, the H-surface

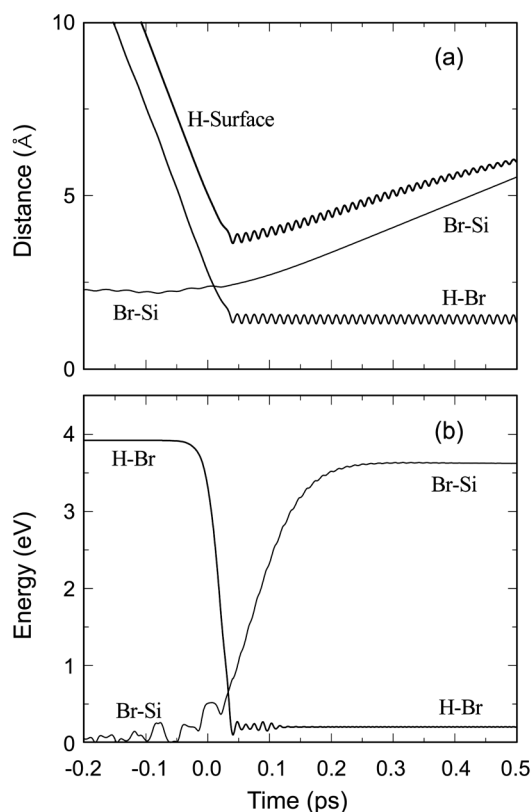


Figure 7. Dynamics of a representative trajectory at (1800, 300 K): (a) Time evolution of the H-surface, H-Br and Br-Si distances. (b) H-Br interaction energy and Br-Si vibrational energy.

distance is the collision trajectory, but the outgoing H-surface distance does not represent the collision trajectory, which now has to be the distance between the center of mass of HBr and the surface. In the outgoing segment, the Br-Si distance shown in the figure better describes the collision trajectory. The time evolution of the H-Br and Br-Si distances clearly show the H-Br bond formation and the Br-Si bond dissociation. Note that after the H atom reaches the closest distance on impact, the Br-Si distance begins to diverge, whereas the H-Br distance undergoes a highly organized vibrational motion near the equilibrium bond distance $r_e = 1.414 \text{ \AA}$. This vibrational motion clearly indicates the formation of a stable product molecule. In this case, the displacement of the Br-Si bond distance from its equilibrium reaches 5 \AA at $t = 0.43 \text{ ps}$, at which time HBr is formed.

The incident gas atom with collision energy E undergoes inelastic interaction with the adatom-surface vibration through the repulsive part of the H to Br potential. This is an important process which produces energy exchange between the H to Br interaction and the Br-Si vibration. In order for the H atom to form H-Br bond on a short-time scale, it must redirect its energy along the reaction coordinate in the early stage of collision. This energy is the primary driver for the reaction and the redirection occurs in the presence of strong attraction between H and Br. When the H to Br interaction loses energy to the Br-Si vibration, the incident gas atom

falls into the H-Br potential well. The high efficiency of this energy transfer process is evident in Figure 7(b), where the H to Br interaction energy decreases sharply from D_{HBr} to the final value $E_{\text{v,HBr}}(\infty) = 0.201$ eV, whereas the Br-Si vibrational energy, $E_{\text{v,BrSi}}(t)$, rises rapidly from its initial value $E_{\text{v,BrSi}}^0$ toward the dissociation threshold $D_{\text{BrSi}} = 3.621$ eV. The comparison of the curves shown in Figures 7(a) and 7(b) reveals important features of intramolecular energy flow and subsequent bond breaking and formation in the reaction taking place on a subpicosecond scale. The sharp rise and fall of these energies during the impact clearly indicate an efficient flow of energy from the newly formed energy-rich H-Br bond to the weakening Br-Si bond in the short-lived surface complex $\text{H}\cdots\text{Br}\cdots\text{Si}$ as a result of a strong collision between H and Br. That is, the transfer of a large amount of vibrational energy occurs in a single-step process rather than a ladder-climbing process in which the Br-Si bond would acquire its energy in a series of small steps. When the H to Br interaction directs sufficient energy to the Br-Si vibration through a strong collision, the Br-Si bond weakens sufficiently so that it can break, thus leading to the binding of the desorbing Br atom with H. For the representative trajectory considered in Figure 7, the reaction energy available for partitioning among various motions in the product state is 0.630 eV. The major portion of this energy deposits in the translational and vibrational motions of HBr [*i.e.*, in the limit $t \rightarrow +\infty$, $E_t(\infty) = 0.248$ eV and $E_v(\infty) = 0.202$ eV]. The amount of energy transferred to the solid is $E_s(\infty) = 0.180$ eV, which is significant. Only a small fraction is found to deposit in the rotational motion: $E_r(\infty) = 0.0012$ eV.

Concluding Comments

We have studied the interaction of gas phase atomic hydrogen with a highly covered chemisorbed bromine atoms on a silicon surface with particular emphasis on the reaction mechanism. The reaction takes place through the ER mechanism, but the extent of HBr formation is not large. The reaction probability is essentially independent of the surface temperature between 0 and 700 K, whereas its dependence on the gas temperature is significant. When the surface temperature is maintained at 300 K, the largest value the reaction probability can take is about 0.07 near the gas temperature of 800 K. All reactive events occur in single collisions *via* a strong interaction between the gas atom and the adatom, leading to the transfer of a large amount of energy to the adatom-surface bond on a subpicosecond scale.

In HBr formation, most of the reaction exothermicity deposits in the translational and vibrational motions of the product molecule and a smaller, but significant amount dissipates into the surface. The upper limit of energy deposited in the translational motion is about 40% of the available energy at the collision conditions considered in the study. The majority of HBr molecules are produced in low-lying vibrational states sharing about 30% to 35% of the available energy. The vibrational population distribution is found to be

statistical. The amount of energy shared by the rotational motion is much smaller, implying that HBr rotation does not play an important role in the desorption process. The surface provides significant energy flow. The amount of energy dissipated into the surface is about 25% of the available energy.

Acknowledgement. This study was financially supported by Chonnam National University. The computational part of this study was supported by “the Eighth Supercomputing Application Support Program” of the KISTI (Korea Institute of Science and Technology Information).

References

1. *Interaction of Atoms and Molecules with Solid Surfaces*; Bortolani, V.; March, N. H.; Tosi, M. P., Eds.; Plenum: New York, 1990.
2. *Dynamics of Gas-Surface Interactions*; Rettner, C. T.; Ashfold, M. N. R., Eds., Royal Society of Chemistry: Thomas Graham House, Cambridge, England, 1991.
3. Somorjai, G. A. *Introduction to Surface Chemistry and Catalysis*; Wiley: New York, 1994.
4. Shustorovich, E. *Surf. Sci. Rep.* **1986**, *6*, 1.
5. Christmann, K. *Surf. Sci. Rep.* **1988**, *9*, 1.
6. *CRC Handbook of Chemistry and Physics*, 64th Ed.; Weast, R. C., Ed.; CRC Press: 1983; pp F176-F181.
7. Koleske, D. D.; Gates, S. M.; Jackson, B. *J. Chem. Phys.* **1994**, *101*, 3301.
8. Kratzer, P. *J. Chem. Phys.* **1997**, *106*, 6752.
9. Ree, J.; Shin, H. K. *J. Chem. Phys.* **1999**, *111*, 10261.
10. Kim, Y. H.; Ree, J.; Shin, H. K. *Chem. Phys. Lett.* **1999**, *314*, 1.
11. Ree, J.; Kim, Y. H.; Shin, H. K. *Bull. Korean Chem. Soc.* **2007**, *28*, 635.
12. Kim, Y. H.; Ree, J.; Shin, H. K. *J. Chem. Phys.* **1998**, *108*, 9821.
13. Lim, S.-H.; Ree, J.; Kim, Y. H. *Bull. Korean Chem. Soc.* **1999**, *20*, 1136.
14. Ree, J.; Chang, K. S.; Moon, K. H.; Kim, Y. H. *Bull. Korean Chem. Soc.* **2001**, *22*, 889.
15. Ree, J.; Yoon, S.-H.; Park, K.-G.; Kim, Y. H. *Bull. Korean Chem. Soc.* **2004**, *25*, 1217.
16. Adelman, S. A. *J. Chem. Phys.* **1979**, *71*, 4471.
17. Tully, J. C. *J. Chem. Phys.* **1980**, *73*, 1975.
18. Radeke, M. R.; Carter, E. A. *Phys. Rev. B* **1996**, *54*, 11803.
19. Huber, K. P.; Herzberg, G. *Constants of Diatomic Molecules*; Van Nostrand Reinhold: 1979; p 278.
20. Lee, J. Y.; Kang, M.-H. *Phys. Rev. B* **2004**, *69*, 113307.
21. Eves, B. J.; Lopinski, G. P. *Surf. Sci.* **2005**, *579*, L89.
22. Ghio, E.; Mattered, L.; Salvo, C.; Tommasini, F.; Valbusa, U. *J. Chem. Phys.* **1980**, *73*, 556.
23. Cheng, C. C.; Lucas, S. R.; Gutleben, H.; Choyke, W. J.; Yates, J. T. *J. Am. Chem. Soc.* **1992**, *114*, 1249.
24. Koleske, D. D.; Gates, S. M. *J. Chem. Phys.* **1993**, *99*, 8218.
25. *American Institute of Physics Handbook*, 3rd ed.; Gray, D. E., Ed.; McGraw-Hill: New York, 1972; pp 4-116.
26. Ree, J.; Kim, Y. H.; Shin, H. K. *J. Chem. Phys.* **1996**, *104*, 742.
27. Eenshuistra, P. J.; Bonnie, J. H. M.; Lois, J.; Hopman, H. *Phys. Rev. Lett.* **1988**, *60*, 341.
28. Takamine, Y.; Namiki, A. *J. Chem. Phys.* **1997**, *106*, 8935.
29. Gates, S. M.; Kunz, R. R.; Greenlief, C. M. *Surf. Sci.* **1989**, *207*, 364.
30. Kratzer, P.; Brenig, W. *Surf. Sci.* **1991**, *254*, 275.
31. Ree, J.; Shin, H. K. *Chem. Phys. Lett.* **1996**, *258*, 239.
32. Lemoine, D.; Quattrucci, J. G.; Jackson, B. *Phys. Rev. Lett.* **2002**, *89*, 268302.
33. Mullins, C. B.; Rettner, C. T.; Auerbach, D. J. *J. Chem. Phys.* **1991**, *95*, 8649.
34. Kim, W. K.; Ree, J.; Shin, H. K. *J. Phys. Chem.* **1999**, *103*, 411.